A numerical investigation of salinity variations in the Barataria Estuary, Louisiana in connection with the Mississippi River and Restoration Activities

Yanda Ou[a], Z. George Xue[a, b, c*], Chunyan Li[a, c], Kehui Xu[a, c], John R. White[a, c], Samuel J. Bentley [c,d], Zhengchen Zang [a]

[a] Department of Oceanography and Coastal Sciences, Louisiana State University, Baton Rouge, LA, 70803, USA

[b] Center for Computation and Technology, Louisiana State University, Baton Rouge, LA, 70803, USA

[c] Coastal Studies Institute, Louisiana State University, Baton Rouge, LA 70803, USA

[d] Department of Geology and Geophysics, Louisiana State University, Baton Rouge, LA, 70803, USA

[*] Corresponding to Z. George Xue (zxue@lsu.edu)

Abstract

A three-dimensional numerical model was applied to the Barataria Estuary in the Northern Gulf of Mexico to study its salinity variations as well as the impacts from the Mississippi River discharges and proposed river diversions. Model-observation comparison showed that the model was able to reproduce the hydrodynamic fields on subtidal to seasonal time scales. Salinity in the Barataria Estuary was high in falls and low in summers, with greater variability in the lower estuary than the upper estuary. While salinity in the upper estuary was controlled by discharges from a local freshwater diversion, salinity in the lower estuary was mostly affected by the mixed Mississippi River water transported via the tidal inlets in the south. The correlation between Mississippi River discharges and estuarine salinity indicated that low salinity Mississippi River water could intrude into the estuary through the middle and east tidal inlets. Sensitivity tests were performed to assess the impacts from the Mississippi River discharges and proposed mid-Barataria Estuary sediment diversion. Model results illustrated that salinity in the estuary was more sensitive to an increased Mississippi River discharge than a decreased one. The proposed mid-Barataria sediment diversion was likely to induce a dramatic

decrease of salinity in the lower estuary. The ecosystem consequences of the fluctuation of Mississippi River discharges as well as that of the proposed river diversions needs further investigation.

1. Introduction

        Saline environments are crucial to the distribution and growth of aquatic organisms. Three biological gradients, i.e., populations of sessile or slightly motile marine organisms, size of motile organisms, and species numbers, are deemed to be closely correlated with salinity gradient in estuaries (Gunter, 1961). For example, the optimum salinity range for natural oyster growth and survival is from 5 to 15 (Galtsoff, 1964). Extremely low salinity (<5) has negative impacts on oyster recruitment, survival and growth (La Peyre et al., 2013).

        The Barataria Estuary in Louisiana is a semi-enclosed water body located right next to the Mississippi "birdfoot" delta (Fig. 1b). The variability of salinity in the Barataria estuary can be largely influenced by man-made structure (like river diversions; Das, 2010; White et al., 2018) and the Mississippi Plume via the tidal inlets along the southern boundary of the estuary (Orlando et al., 1993; Li et al., 2011). Before the construction of the Davis Pond freshwater diversion (DPFD), long-term averages of observed near-surface salinity at the Grand Terre (at Pass Abel, see Fig. 1d) and St. Mary's Point (station reference number 317 by the Louisiana Department of Wildlife and Fisheries, near USGS6 shown in Fig. 1a) were 20.90 and 12.90, respectively (Wiseman and Swenson, 1989; Wiseman et al., 1990). There is a remarkable salinity gradient in the estuary with relatively low salinity in the northern estuary and high in the southern part. In the northern estuary, mean salinity ranged from 0 to 3, while in the middle and southern parts, the ranges were from 3 to 9 and from 9 to 22, respectively (Wiseman and Swenson, 1989). On the other hand, salinity at Grand Terre exhibited a fall of 0.007 per month over the period of 1961 to 1974, which was deemed to be correlated with the increased Mississippi River discharge (Van Sickle et al., 1976). Orlando et al.(1993) reported that the months-to-seasons variability of salinity across the Barataria Estuary was dominated by shelf processes especially when Mississippi River inflow was high.

        Ever since its first operation in 2002, DPFD has resulted in pronounced decreases in annual mean salinity values across the entire estuary (White et al., 2018). The DPFD diverts freshwater from the Mississippi River in the north to the estuary at an average rate of 40 m^3/s . Park (2002) and Inoue et al. (2008) applied integrated hydrology–hydrodynamic model to the Barataria Estuary showing that during a dry summer (in 1999), freshwater release could bring notable impacts on salinity in the mid-estuarine region. Another model simulations by Das (2010) pointed out that the effects of DPFD discharges were most apparent in the middle and lower

estuary. However, using a multi-variable linear model, Swenson (2003) suggested that the salinity at the middle and lower Barataria was sensitive to the Mississippi river discharges. Model results by White et al. (2018) indicated that salinity in the upper Barataria Estuary was sensitive to the DPFD, whereas the lower basin was sensitive to the proposed mid-Barataria sediment diversion (MBSD). And the impacts from Mississippi River via the tidal inlets in the south probably overwhelmed any impacts from the operation of DPFD. A most recent hydrodynamical study of the Barataria Bay suggested that the exchange flows in and out of the bay were highly dependent on weather systems and associated winds (Li et al., 2019). Along coastal Louisiana, tides are dominated by diurnal constituents (Kantha, 2005) with a maximum tidal range of ~ 0.6 m (Harris, 1981; Forbes, 1988). However, currents converge at narrow tidal passes and could reach ~1.3 m/s at the Barataria Pass (Li et al., 2011). During cold front events, the ratios of subtidal transports through the four major inlets varied substantially with 18% ± 13%, 35% ± 18%, 31% ± 16%, and 16% ± 9% for Caminada Pass, Barataria Pass, Pass Abel, and Quatre Bayou Pass, respectively (Li et al., 2019; Li 2013). The subtidal transports through the inlets can have a substantial impact on salinity in the lower estuary. Most recently, Juarez et al. (2020) performed a statistical analysis on saltwater distribution in Barataria Bay and reported a salt plug (i.e. water somewhere in the estuary with higher salinity than the ocean), which was affected by both estuarine dynamics and discharge from the Mississippi River.

A quantitative assessment of the impacts of DPFD (in the north) and the Mississippi River inflow (from the south) on the salinity in the estuary is still not available. In addition, there are still lack of studies of the spatiotemporal variability of estuary salinity. Existing studies primarily focused on the impacts of DPFD, whereas failed to exam or quantify the impacts from the Mississippi River. Although White et al. (2018) pointed out that the influences of the Mississippi River could be more important than that of the DPFD, no further evidence was provided. To make the situation even more complicated, the proposed MBSD project is likely to impose further uncertainty to the salinity distribution. The objectives of this study are to investigate the spatial and seasonal variability of salinity in the Barataria Estuary, followed by a quantitative assessment of the impacts from the Mississippi River flows and restoration projects (the existing DPFD and planned MBSD).

2 Method

2.1 Study area

The Barataria Estuary has an area of approximately 6,300 km^2 (Park, 2002; Habib et al., 2007) and is an important oyster habitat with an average yield of 7,562.5 barrels per year during the period of 1976- 2016 (Louisiana Department of Wildlife and Fisheries, 2019). Tide in this area is weak with microtidal ranges and is mainly controlled by diurnal tide systems (Li et al., 2018; Li et al., 2011). The estuary is shallow and well-mixed with an averaged depth of 2 meters (Das et al., 2012; Li et al., 2011; Cui et al., 2018) and is bounded by the bank of the Mississippi River to the north and east, Bayou Lafourche to the west, and the northern Gulf of Mexico (nGoM) to the south (Park, 2002). The estuary consists of a series of lakes and small bays including near-fresh water lakes like Lake Cataoutche and Lake Salvador in the northern part, and saline water ones like Little Lake and the Barataria Bay in the middle and southern part, respectively (Fig. 1a). By far, the most important freshwater input is from the man-made DPDF, which diverts the Mississippi River water from the channel to the estuary in the north. The averaged DPDF discharge was 40 m^3/s from 2014 to 2018, with a maximum value of 610 m^3/s. The salinity in the middle and southern part can be affected by the shelf water intrusion through several tidal inlets. Low saline water coming from the Mississippi River mouth can be transported by the westward longshore currents and invade into the lower estuary during high discharge periods (Orlando et al., 1993).

2.2 Numerical model set-ups and available measurements

We adapted a 3-dimensional, free surface, topography following numerical model -- the Regional Ocean Model System (ROMS,version 3.7) to the Barataria Estuary. ROMS solves finite difference approximations of Reynolds Averaged Navier-Stokes equations applying hydrostatic and Boussinesq approximation with a split explicit time stepping algorithm (Haidvogel et al., 2000; Shchepetkin and McWilliams, 2005, 2009). As a state-of-the-art regional ocean model, ROMS has been widely applied to aquatic environment of different spatial scales, from basin-wide ocean circulation (e.g., Haidvogel et al., 2000), and shelf circulation (e.g., Marchesiello et al., 2003), to estuarine salt balance variations (e.g., Maccready et al., 2002; Maccready and Geyer, 2001; Warner et al., 2005; Li et al., 2005).

Our model used a curvilinear coordinate with a horizontal resolution of ~ 200 m and eight vertical sigma layers. The model hindcast covered the period of August 1, 2012- June 30, 2018. We selected this period mainly because of the availability of in-situ data. The first 17 months were regarded as a spin-up and the analysis presented below was based on the results from January 1, 2014 to June 30, 2018. The wetting and drying scheme (Warner et al., 2013) was applied to the model for a more accurate simulation in shallow waters. The computational time step (i.e. baroclinic time step) was set to be 20 seconds and the number of barotropic time steps between each baroclinic time step was set to be 5. Model results were outputted on an hourly interval.

The south boundary was the only open boundary and was forced by hourly water level, 3-D current velocity components, depth-integrated horizontal current velocity components, 3-D salinity and temperature. The boundary water levels were derived from the tidal station at Grand Isle, LA (073802516 Barataria Pass) maintained by U.S. Geological Survey (USGS) National Water Information System (NWIS). Other boundary conditions were derived from a parent nGoM with a horizontal resolution of 1 km (see Zang's et al. 2019 for details of model setup and validation). For lateral boundary conditions we utilized Chapman implicit for free surface or water level (Chapman, 1985), Flather for 2-D momentum (Flather, 1976), gradient for mixing total kinetic energy, and mixed radiation-nudging condition for 3-D momentum, temperature and salinity (Marchesiello et al. 2001). To better resolve tidal influences, the nudging time steps for the 3-D momentum, temperature and salinity were set to 1 hour for inflow and 60 days for outflow. Boundary nudging technique was performed at the computational grids along the open boundary. We chose a one-way nesting instead of a two-way nesting because previous studies indicated that hydrodynamics to the south of the Barataria barrier island chain (i.e. around the Bird's Foot Delta and Louisiana Bight) were mainly driven by the Mississippi River plume and winds (Li et al., 2011). Impacts from the estuary were limited around the inlets (Li et al., 2019).

Instantaneous measurements of DPFD discharges were added to the model as point sources on the northern boundary near Lake Cataoutche with a 15-minutes interval (the 10 red dots in the northernmost shown in Fig. 1a). The DPFD transported horizontal momentums and freshwater to the study domain. The discharge measurements were obtained from site 295501090190400 near Boutte, LA provided by the USGS NWIS and covered the time period of 2012-2018. The magnitude of river discharges was multiplied by 1.4 to account for adjacent

watershed areas and lateral inflow of tributaries (Warner et al., 2005). Six-hourly atmospheric forcings, including net longwave radiation flux, net shortwave radiation flux, precipitation rate, surface air temperature, surface air pressure, and surface relative humidity, were derived from the NCEP Climate Forecast System Version 2 with a horizontal resolution of 22 km (Saha et al., 2011). Hourly wind fields were retrieved from station 8761724, Grand Isle, LA operated by the NOAA/ National Ocean Service. The wind forcing was spatially uniform over the computational domain.

Hourly water level, near-surface temperature, and near-surface salinity at 11 sites in the estuary provided by the USGS NWIS were used for model validation. These sites covered a large area of the estuary from the Lake Cataoutche in the northernmost to the Little Lake in the middle and the Barataria Bay in the lower estuary (black crossing signs in Fig. 1a). We renamed the USGS sites out of simplification (see Table 1 for details). Most of the observations covered the entire study period (2014-2018), which enabled high-quality model validations described in section 3. In addition, hourly near-surface current velocity measurements by an Acoustic Doppler Current Profiler (ADCP) in the Barataria Pass were also available (Li et al., 2019). The ADCP instrument was mounted on east edge of the Barataria Pass at about 3 m below the sea surface looking perpendicular to the along-channel direction. The velocity series covered a length of a month from July 27, 2015 to August 28, 2015. The coordinate system was rotated counterclockwise by 52.7° to obtain the along‐channel and cross‐channel velocity components (Li et al., 2011). A positive along-channel velocity was corresponding to transports into the bay.

3 Model Validation

3.1 Water level

Hourly water level measurements varied from -0.5 to 1.2 m (Fig. S1~S3) relative to the NAVD88 datum. Variation of water level exhibited salient diurnal cycles at the 11 sites. Time series of model simulated water levels agreed well with the observations, with the correlation coefficients ranging from 0.72 to 0.96 at stations with 4.5-year records (> 35883 records, Fig. S1~S2) and higher than 0.90 at stations with 8-month records (> 5768 records, Fig. S3) . The averaged bias and root mean square error (RMSE) between simulated and observed water level ranged from -0.08 to 0.09 m and from 0.05 to 0.14 m, respectively. The maximum bias and

maximum RMSE were 0.09 m at site USGS7 and 0.14 m at site USGS6, respectively. Tidal effects were weakened as tides propagated northward into the estuary. The diurnal tidal signals were the weakest at site USGS1, which was located northernmost of the estuary.

3.2 Surface temperature and surface salinity

Observed sea surface temperature (SST) ranged from 1.5 °C to 35.0 °C, exhibiting pronounced diurnal and seasonal cycles at the 11 sites (Fig. S4~S6). Simulated SST time series captured the overall variations of the measurements, showing pronounced seasonal cycles and remarkable daily fluctuations. The correlation coefficients between simulations and measurements were equal to or greater than 0.96 at all stations (Fig. S4~S6). Averaged biases (from -0.95 to 1.19 °C) were small compared to the magnitude of measured SSTs. Correspondingly, the RMSEs were all less than 2.53 °C with the highest value found at site USGS1. Simulated SSTs at the upper and middle estuary were slightly lower than the measurements, while those at the lower estuary were slightly higher than the measurements.

The model was not able to capture the peak values of sea surface salinity (SSS) at the upper estuary, especially at site USGS2 (Fig. S7b) and site USGS3 (Fig. S7c). The underestimation of SSS might be caused by the resolution of model's bathymetry data, which would impede the intrusive saltwater from the south via the narrow channels. The other possibility could come from the overestimated mixing processes, which could be potentially resolved by adding more vertical layers to the model. During nearly 95% and 89% of time, observed SSS at site USGS2 and USGS3 were lower than 5, respectively. Our model reproduced the SSS well at these two sites when SSS were below 5. In the middle and lower estuary (Fig. S7d, Fig. S8~S9) where tidal effects were pronounced, the correlation coefficients were relatively higher, ranging from 0.54 to 0.75 at stations with 4.5-year records (Fig. S7d, Fig. S8) and from 0.71 to 0.87 at stations with 8-month records (Fig. S9). Site USGS6 had the highest bias (4.97) and the highest RMSE (6.67). SSS in the lower estuary exhibited a more salient annual cycle than those in the upper estuary, indicating that mechanisms of salinity variability could be quite different in these two areas. As our study focuses on the seasonal variability of salinity, a low-pass filter (Emery and Thomson, 2001) was applied to both the simulated and observed SSS time series to extract subtidal signals. The cut-off frequency was 1/48 hour^{-1}. Similar results could be found in before- and after-filtered series, yet with slightly higher

correlation coefficients for the latter in the lower estuary (Fig. S11~S12). Our model is capable of reproducing the salinity variability on subtidal to seasonal scales at the 11 sites.

3.3 Near-surface current velocity

Along-channel near-surface current velocity measured by the ADCP was approximately one order of magnitude larger than the cross-channel component (figure not shown). The exchanges of water and materials between the estuary and shelf were mainly driven by the along-channel component (Li et al., 2011). We compared the along-channel velocity component between simulation and measurement (782 records) in Fig. S13. The correlation coefficient is 0.59 (above 99% confidence level). The mean bias and RMSE were 0.05 m/s and 0.38 m/s, respectively. The model was not able to capture the peak velocity. The model-data discrepancy was likely caused by the relatively coarse grid resolution (~200 m). Nevertheless, considering the ADCP was positioned at the edge of the Barataria Pass, which is 600 m in width, the observed velocity might not represent the full scenario of the flux at the pass.

4 Results

4.1 Multi-year mean salinity

The Barataria Estuary is a well-mixed estuary (Das et al., 2012; Li et al., 2011; Cui et al., 2018). Multi-year mean (January 1, 2014 ~ January 1, 2018) water density differences between near-bottom and near-surface layers was generally lower than 1.4 kg/m^3 over 99% of the computational grids inside the estuary. The only exception was found in regions near the Barataria Pass where the values were approximately 2.0 kg/m^3 (Fig. 2a). Accordingly, the majority of the estuary was considered to be well-mixed, and all following analysis was conducted based on the depth-averaged variables of interests.

Multi-year mean of depth-averaged salinity increased gradually from 0 at the head of the estuary to about 23.0 around the barrier island chain (Fig. 2b), which was consistent with the observations by Wiseman and Swenson (1989) and Wiseman et al. (1990). The mean depth-averaged salinity over the entire estuary was 11.7. In the middle estuary, salinity started to increase sharply near the isohaline of 8 as depicted by the solid red line in Fig. 2b. To the north of this isohaline, the salinity maintained low and showed little spatially variability. Nevertheless, salinity gradient became pronounced to the south of the isohaline of 8. In the next we used the

isohaline of 8 as the boundary of the upper and lower estuary. The multi-yearly averaged wind speed over the studied domain was 0.91 m/s from the northeast. Wind speeds were deemed to be highly correlated to the hydrodynamical fields in the Barataria Bay on weather scales, e.g. cold fronts (Li et al., 2013, 2019) and were responsible for the annual variability of salt-plug in the bay (Juarez et al., 2020). Depth-averaged currents outside the estuary were westward along the barrier island chain. These westward currents were able to bring the relatively fresh water from the Mississippi plume in the southeast to the estuary through tidal inlets like Grand Bayou Pass (Orlando et al., 1993). The westward along-coastline currents could also introduce saltwater intrusions from the shelf when Mississippi discharge is low.

4.2 Seasonal variability of salinity

The multi-year mean salinity exhibited limited spatial variations over different seasons (Fig. 2c~2f). Here, March, April, and May were defined as spring months; June, July, and August were defined as summer months; September, October, and November were defined as fall months; and December, January, February were defined as winter months. The magnitude of salinity and location of the isohaline of 8 differ over seasons. In springs, the spatially averaged salinity over the entire estuary was 10.7. In summers, the salinity reached the lowest with a mean value of 9.5. The location of isohaline of 8 was further southward. During falls, the mean salinity reached its maximum (13.9). The isohaline of 8 reached further northward than in other seasons. The winter mean salinity was 12.6, which was the second highest. Salinity in the uppermost estuary (mainly the waters north of the isohaline of 8) remained nearly unchanged despite of variations in DPFD discharges. The coastal currents along the barrier island chain flowed westward throughout a year.

The time series of spatially averaged daily salinity for the upper, lower, and entire estuary were shown in Fig. 3. Averaged salinity in the estuary ranges from 6 to 18 and exhibited an annual cycle with lower salinity in springs and summers and higher value in late falls and early winters (Fig. 3b). Salinity over the upper estuary did not exhibit remarkable annual cycles but could fluctuate dramatically between 0.2 to 6 within days (Fig. 3a). Throughout the period of interest, the upper-estuarine salinity was 1.4 on average, while the standard deviation (STD) was 1.1, which was about 79% of the mean value. Similar as that of the entire estuary, the lower-estuarine salinity was relatively high in late falls and early winters and low in summers (Fig. 3b).

Thus, salinity variations of the entire estuary were mainly from those of the lower estuary rather than those of the upper estuary. However, the magnitude of the lower-estuarine salinity (ranging from 9 to 26) was greater than that of the entire estuary. When compared to the upper-estuarine salinity, the fluctuation for the lower-estuarine salinity was smaller with a STD of 4.1, which was only 24% of its mean value (17.4).

4.3 Davis Pond diversion

The DPFD discharge did not change "naturally" with time but acted like episodic and pulsed injections without a significant annual cycle (Fig. 3a). During over 80% of the time, the daily mean discharges were kept below 60 m^3/s. However, in certain periods of a year the discharge could increase by 4 to 5 folds, reaching 300 m^3/s. The STD of the DPFD discharges was 42.1 m^3/s, which was comparable with its mean value (40.7 m^3/s). The variability of salinity in the upper estuary was very sensitive to the changes of the DPFD discharges. The peaks/troughs of the discharges usually led the troughs/peaks of the salinity by 10-30 days.

We introduced lead/lag correlation coefficients (CCs) to exam the correlations between river discharges and salinity with phase delays. The lead/lag CCs represent the time series leads/lags the other time series by a certain length of time. Lead/lag CCs of the DPFD discharges and salinity in the upper estuary reached the highest when the discharges led by 10-35 days (Fig. 4a). Nevertheless, the maximum CC was only -0.44, which implied a moderate correlation between the two time series. Spatially, the CCs attained the highest value (~ -0.45, above 99% significant level) in the middle and southwestern part of the estuary when the discharges led by 35 days (Fig. 4b). The CCs in Lake Cataouatche and Lake Salvador were much lower (-0.30 ~ -0.20). SSS observations at site USGS1 in Lake Cataouatche were almost constant during the investigated period (Fig. S7a). The variations of DPFD discharges affected the salinity fluctuation mostly in the middle and southwestern side of the estuary. Such results were consistent with previous studies (Park, 2002; Inoue et al., 2008; Das, 2010).

We concluded that the time series of upper-estuarine salinity contained two signals: nearly unchanged salinity values in the two lakes upper most of the estuary and fast changing values in mid- and southwest part of the estuary. The variability of the latter was moderately modulated by the DPFD.

11

4.4 Mississippi River

The high-quality continuous measurements at site 07374000, Baton Rouge, LA were used to estimate the Mississippi River discharges. Time series of river discharges reached the highest in springs and lowest in falls (Fig. 3b). The troughs (peaks) of the discharges led the peaks (troughs) of the lower-estuarine salinity by approximately 30 days.

Lead/lag CCs of Mississippi River discharges and lower-estuarine salinity reached the maximum of -0.60 over the 99% confidence level when the discharges led by 28 days (Fig. 4c). The distribution map of CCs depicted that salinity in the southeastern part of the lower estuary was significantly correlated with the Mississippi River discharges with the coefficients ranging from -0.65 to -0.50 (Fig. 4d). This suggested that Mississippi River freshwater could intrude into the estuary through the middle passes (Pass Abel and Quatre Bayou Pass), and the east passes (e.g. Grand Bayou Pass).

5 Discussion

Our model results exhibited the seasonal variability of salinity in the Barataria Bay. Time series analysis built on river discharge and model results confirmed salinity in the lower estuary is dominated by the Mississippi River water from the south. In this section we discuss how differences in Mississippi River discharges and the proposed river diversion project is likely to alternate the salinity field in the estuary.

5.1 Mississippi River discharge

A recent study by Zang et al. (2019) identified a significant decrease (~18%) in Mississippi River discharge in the period of 1999-2012, which was ascribed to the phase shift of ENSO from the strong El Niño episode of 1997/98 to the strong La Niña episode of 1999/2000 (Zang et al., 2019; Twine et al., 2005). To assess the magnitude of the impacts from the Mississippi River discharge on estuarine salinity, we halved and doubled the Mississippi River discharges in the "parent" nGoM model, respectively and reran the nGoM model to generate two new sets of open boundary conditions for the Barataria model. We then rerun the Barataria model with all parameters and physical setups identical to the standard run described in section 2.2, but with different open boundary conditions.

The salinity differences between the half-Mississippi scenario and the standard scenario exhibited pronounced seasonal variations (Fig. 5a~5d), with the greatest changes in winters, and

the least in summers. The impacts of the halved Mississippi River discharges on the salinity distribution showed great spatial differences. The averaged increases of salinity over the lower estuary ranged from approximately 2.1 to 2.7, while the increases in the upper part were limited within 1.0. It was also worth to note that salinity could also be decreased remarkably in the western lower estuary in summers, in the middle lower estuary in winters, and in the eastern lower estuary in falls. It could be explained by the changes of the relative contribution from the Mississippi River discharges and Davis Pond discharges when the former was halved. Correlation coefficient between the halved Mississippi River discharges (leading by 28 days) and the corresponding estuarine salinity gave high CC values in the entire lower estuary ranging from -0.75 to -0.50 (Fig. 6). For the standard case, the corresponding coefficients ranged from -0.65 to -0.50 only significantly in the southeastern part of the lower estuary (Fig. 4d). The seasonality of competition between river discharges could therefore behaved differently in standard and half-Mississippi scenarios, which needs further investigations and is beyond the scope of this study.

In comparison with the standard scenario, once the Mississippi River discharges were doubled, salinity decreased almost over the entire estuary (Fig. 5e~5h). Averaged decreases fluctuated from 5.6 to 7.5 over the lower estuary and ranged from 0.7 to 1.3 over the upper part. Salinity was slightly elevated in the western lower estuary in winters. Like the halved-Mississippi scenario, salinity differences also showed seasonality, especially in the lower estuary. The greatest salinity decreases occurred in summers when the Mississippi River discharge peaked, while the least salinity decreases happened in winters when the discharge was minimum.

The salinity in the upper estuary barely changed in the two sensitivity tests, confirming that the impacts from Mississippi discharge were limited in the lower estuarine. The impacts of Mississippi River discharge on the estuarine salinity were more pronounced in the doubled discharge scenario. Daily time series comparisons also showed that spatially averaged salinity over the entire estuary exhibited more pronounced decreases (-39%) in the doubled-Mississippi scenario (Figs. 7a and 7b), but less increases for the halved-Mississippi scenario (Fig. 7a) with an averaged percentage change of +17% (Fig. 7b). The percentage of salinity change in difference seasons followed that of the Mississippi River discharges, especially for the doubled-Mississippi scenario. Results of the two sensitivity tests implied that the ecosystem in the estuary, especially the lower portion, would be more vulnerable in an abnormally wet year (high Mississippi discharge) than a dry year. Aquatic organisms, especially the sessile organism would possibly

experience a higher mortality rate due to stronger freshwater intrusion when the Mississippi discharge is maximum in the wet seasons (e.g. springs and summers).

5.2 Mid-Barataria sediment diversion

The Barataria Basin is suffering a loss of 1,300 acres of coastal wetlands every year (Couvillion et al., 2017). Proposed by U.S. Army Corps of Engineers, the MBSD system has been under construction since 2017 with an aim to slow down the land losing processes by diverting sediments from the Mississippi River to the mid-Barataria estuary. However, there is still a lack of study assessing the possible impacts of this diversion system on the salinity variability in the estuary. The proposed discharges of the MBSD will be determined according to the Mississippi River flows at the USGS gage at Belle Chasse, Plaquemines Parish, Louisiana (Gulf Engineers & Consultants, 2018; CPRA, 2017). The MBSD would discharge up to 2,123.76 m^3/s of freshwater together with sediments and nutrients into the mid-Barataria Basin when Mississippi River flows are 12,742.58 m^3/s or greater but would maintain a base flow of up to 141.58 m^3/s when the Mississippi River flows are below 12,742.58 m^3/s (Gulf Engineers & Consultants, 2018). We performed another sensitivity test by adding the MBSD as point sources (the 30 red dots in the middle estuary shown in Fig. 1a) to the mid-estuary with a discharge being either 141.58 m^3/s or 2123.76 m^3/s depending on the Mississippi River flows. The MBSD discharge was equally distributed at all the point sources. During 70% and 30% of time, the MBSD discharges were 141.58 m^3/s and 2,123.76 m^3/s, respectively. The salinity of the MBSD outflows was set to be 0.2 which was the same as DPFD outflows. In the sensitivity test the MBSD introduced both momentum and fresh water to the estuary.

The operation of MBSD would lead to a remarkable salinity reduction, especially in the lower estuary, throughout a year (Fig. 5i~5l). In springs/falls, the freshening effects reached its maximum/minimum with a decrease of 13.0/9.2 over the lower estuary. Summers and winters were the secondary and thirdly affected seasons with mean salinity drops of 11.8 and 11.6, respectively. No pronounced salinity change was detected in waters outside of the estuary (south of the tidal inlets). Time series of the depth-averaged salinity over the entire estuary showed a similar annual cycle with that of the standard run (Fig. 7a). Nonetheless, the salinity of the MBSD scenario exhibited a wider range of magnitude, fluctuating between 0.8 to 12.5, and maintained lower than 5 during 68% of simulation time. The averaged percentage change of

14

salinity was -68%, which was much more remarkable than that in doubled-Mississippi scenario (Fig. 7b). The time series of percentage changes was negatively correlated to the Mississippi River discharges since the discharges of the MBSD were determined by the former. Thus, we did see seasonal variations in the time series of percentage changes with the greatest decrease in springs and summers when the Mississippi River discharges peaked, but with the least decrease in falls and winters when the discharges reached the trough. The reduced salinity and elevated frequencies of low-saline conditions would bring a substantial impact on the aquatic ecosystem in the estuary. The days with favorable conditions for oyster recruitment, survival and growth could encounter a dramatic decrease once MBSD is operated. And the prolonged low salinity conditions would shift the Barataria Estuary from a salt marsh-favorable to a fresh marsh-favorable environment.

The Mississippi River is like a 'leaking pipe'. Some water could leak through the levees near Barataria Bay and adds freshwater into the model domain. These line sources were not included in the model. Additionally, the ground water exchanges among river channels, wetland and bays were neglected. Intended consideration of the freshwater sources listed above would probably lead to a fresher estuary than we could predict in the model, especially in the lower part. In order to resist the pronounced salinity reduction in the estuary as the MBSD is operated, managers may need to limit the Mississippi River discharges from the main channel. However, the manipulation could in turn bring side-effects to the watershed.

6. Conclusion

A 3-dimensional numerical model was applied to Barataria Estuary to study its salinity variations from January 1, 2014 to June 30, 2018. Model validation results indicated that the model hindcast was able to reproduce the water level, surface temperature, and surface salinity in the estuary with high correlation coefficients, low average bias, and low average RMSE.

The estuary was well-mixed based on the distribution of density differences between the near-bottom layer and the near-surface layer. Depth-averaged salinity in the estuary reached the highest in falls and lowest in summers. Heavily influenced by freshwater from the Davis Pond freshwater diversion, salinity in the upper estuary maintained lower than 5 during the most of simulation time with no pronounced annual cycle. The Davis Pond freshwater diversion had a

moderate impact on the salinity variability in the middle and southwestern part of the lower estuary with a maximum correlation coefficient of -0.45.

The salinity variability of the Barataria Estuary was mainly controlled by that of the lower estuary. The latter was mainly modulated by the Mississippi River discharges with the highest correlation coefficients between the two ranging from -0.65 to -0.50 over the southeastern part of the lower estuary. The Mississippi River freshwater could intrude into the estuary through the middle passes (Pass Abel and Quatre Bayou Pass), and the east passes (Grand Bayou Pass).

Two sensitivity tests were conducted to assess estuarine salinity's response to the changes in Mississippi River discharges. Salinity in the lower estuary increased by 2.1 ~ 2.7 and decreased by 5.6 ~ 7.5 when Mississippi River discharge was halved and doubled, respectively. The impacts from elevated Mississippi River discharges were more apparent than that from decreased discharges, indicating the ecosystem in the lower estuary was more vulnerable during wet seasons (e.g. springs and summers).

Another sensitivity test was added to project the impact from the proposed mid-Barataria Bay sediment diversion. Results showed that the lower estuary will be the mostly affected area with a salinity drop of 13.0, 11.8, 9.2, and 11.6 for spring, summer, fall, and winter, respectively. With the introduction of the diversion project, the estuarine salinity was lower than 5 during ~ 68% of time. Such dramatic changes in salinity would bring large uncertainty to the aquatic ecosystem.

Reference:

Chapman, D. C. 1985. Numerical Treatment of Cross-Shelf Open Boundaries in a Barotropic
   Coastal Ocean Model. J. Phys. Oceanogr. 15: 1060–1075. https://doi.org/10.1175/1520-
   0485(1985)015<1060:NTOCSO>2.0.CO;2.

Couvillion, B. R., Beck, H., Schoolmaster, D., Fischer, M. 2017. Land Area Change in Coastal
   Louisiana (1932 to 2016). Scientific Investigations Map 3381.
   http://pubs.er.usgs.gov/publication/sim3381.

CPRA. 2017. Louisiana's Comprehensive Master Plan for a Sustainable Coast. Coastal
   Protection and Restoration Authority of Louisiana, Baton Rouge, LA. pp. 171.

Cui, L., Huang, H., Li, C., Justic, D. 2018. Lateral Circulation in a Partially Stratified Tidal Inlet.
   Journal of Marine Science and Engineering 6(4): 159. https://doi.org/10.3390/jmse6040159.

Das, A. 2010. Modeling the Impacts of Pulsed Riverine Inflows on Hydrodynamics and Water
   Quality in the Barataria Bay Estuary. Louisiana State University Doctoral Dissertations.
   1266. https://digitalcommons.lsu.edu/gradschool_dissertations/1266.

Das, A., Justic, D., Inoue, M., Hoda, A., Huang, H., Park, D., 2012. Impacts of Mississippi River
   Diversions on Salinity Gradients in a Deltaic Louisiana Estuary: Ecological and
   Management Implications. Estuarine, Coastal and Shelf Science 111: 17–26.
   http://dx.doi.org/10.1016/j.ecss.2012.06.005.

Emery, W. J. and R. E. Thomson. 2001. Data Analysis Methods in Physical Oceanography.
   Elsevier Science, Chapter 5: Time-series Analysis Methods, Pages 533-539.

Flather, R. A. 1976. A tidal model ofthe northwest European continental shelf. Mémoires
   Société Royale des Sciences de Liège 10: 141–164.

Galtsoff, P. S., 1964. The American oyster, Crasostrea virginica Gmelin. Fishery. Bulletin, 64.
   United States Government Printing Office, Washington, D. C. iii. 480 pp.
   https://doi.org/10.4319/lo.1966.11.2.0312.

Gulf Engineers & Consultants. 2018. Mid-Barataria Sediment Diversion Project Final Scoping
   Report, prepared for US Army Corps Engineers New Orleans District.

Gunter, Gordon. 1961. Some Relations of Estuarine Organisms To Salinity. Limnology and

Oceanography 6(2): 182–90. https://doi.org/10.4319/lo.1961.6.2.0182.

Habib, E., Nuttle, W. K., Rivera-Monroy, V. H., Gautam, S., Wang, J., Meselhe, E., Twilley, R. R. 2007. Assessing Effects of Data Limitations on Salinity Forecasting in Barataria Basin, Louisiana, with a Bayesian Analysis. Journal of Coastal Research 233: 749–63. http://www.bioone.org/doi/abs/10.2112/06-0723.1.

Haidvogel, D. B., Arango, H. G., Hedstrom, K., Beckmann, A., Malanotte-Rizzoli, P., Shchepetkin, A. F. 2000. Model Evaluation Experiments in the North Atlantic Basin: Simulations in Nonlinear Terrain-Following Coordinates. Dynamics of Atmospheres and Oceans 32(3-4): 239-281. https://doi.org/10.1016/S0377-0265(00)00049-X.

Inoue, M., Park, D., Justic, D., Wiseman, W. J. 2008. A High-Resolution Integrated Hydrology-Hydrodynamic Model of the Barataria Basin System. Environmental Modelling and Software 23(9): 1122–32. https://doi.org/10.1016/j.envsoft.2008.02.011.

Juarez, B., Valle-Levinson, A., Li, C. 2020. Estuarine salt-plug induced by freshwater pulses from the inner shelf. Estuarine, Coastal and Shelf Science 232: 106491. https://doi.org/10.1016/j.ecss.2019.106491.

La Peyre, Megan K., Benjamin S. Eberline, Thomas M. Soniat, and Jerome F. La Peyre. 2013. "Differences in Extreme Low Salinity Timing and Duration Differentially Affect Eastern Oyster (Crassostrea Virginica) Size Class Growth and Mortality in Breton Sound, LA." Estuarine, Coastal and Shelf Science 135: 146–57. http://dx.doi.org/10.1016/j.ecss.2013.10.001.

Li, C., 2013. Subtidal Water Flux through a Multi-inlet System: Observations Before and During a Cold Front Event and Numerical Experiments, J. Geophys. Res. Oceans 118: 1877-1892. https://doi.org/10.1002/jgrc.20149.

Li, C., Huang, W., Milan, B. 2019. Atmospheric Cold Front Induced Exchange Flows through a Microtidal Multi-inlet Bay: Analysis using Multiple Horizontal ADCPs and FVCOM Simulations, Journal of Atmospheric and Oceanic Technology, 36: 443-472. https://doi.org/10.1175/JTECH-D-18-0143.1

Li, C., White, J. R., Chen, C., Lin, H., Weeks, E., Galvan, K., Bargu, S. 2011. Summertime Tidal

Flushing of Barataria Bay: Transports of Water and Suspended Sediments. Journal of Geophysical Research: Oceans 116(4): 1–15. https://doi.org/10.1029/2010JC006566

Li, M., Zhong, L., Boicourt, W. C. 2005. Simulations of Chesapeake Bay Estuary: Sensitivity to Turbulence Mixing Parameterizations and Comparison with Observations. Journal of Geophysical Research: Oceans 110(12): 1–22. https://doi.org/10.1029/2004JC002585.

Louisiana Department of Wildlife and Fisheries. 2019. Louisiana Oyster 2017 Stock Assessment Report of the Public Oyster Seed Grounds and Reservations of Louisiana. Oyster Data Report Series No. 23

Maccready, P., and Geyer, W. R. 2001. Estuarine salt flux through an isohaline surface. J. Geophys. Res 106(C6): 11629–11637. https://doi.org/10.1029/2001JC900006.

MacCready, P., Hetland, R. D., Geyer, W. R. 2002. Long-Term Isohaline Salt Balance in an Estuary. Continental Shelf Research 22(11–13): 1591–1601. https://doi.org/10.1016/S0278-4343(02)00023-7.

Marchesiello, P., McWilliams, J. C., Shchepetkin, A. 2001. Open boundary conditions for long-term integration of regional ocean models. Ocean Modelling 3: 1-20. https://doi.org/10.1016/S1463-5003(00)00013-5.

Marchesiello, P., McWilliams, J. C., Shchepetkin, A. 2003. Equilibrium Structure and Dynamics of the California Current System. Journal of Physical Oceanography 33(4): 753-783. https://doi.org/10.1175/1520-0485(2003)33<753:ESADOT>2.0.CO;2.

Orlando, S.P., Rozas, Jr. L.P., Ward, G.H., Klein, C.J. 1993. Salinity Characteristics of Gulf of Mexico Estuaries. National Oceanic and Atmospheric Administration, Office of Ocean Resources Conservation and Assessment: 209.

Park, D. 2002. Hydrodynamics and Freshwater Diversion within Barataria Basin. Louisiana State University Doctoral Dissertations. 980. https://digitalcommons.lsu.edu/gradschool_dissertations/980.

Saha, S., Moorthi, S., Wu, X., Wang, J., Nadiga, S., Tripp, P., Behringer, D., Hou, Y. T., Chuang, H., Iredell, M. NCEP Climate Forecast System Version 2 (CFSv2) 6-Hourly Products; Research Data Archive at the National Center for Atmospheric Research, Computational

and Information Systems Laboratory: Boulder, CO, USA, 2011.

Shchepetkin, A. F., and McWilliams, J. C. 2005. The Regional Oceanic Modeling System (ROMS): A Split-Explicit, Free-Surface, Topography-Following-Coordinate Oceanic Model. Ocean Modelling 9(4): 347-404. https://doi.org/10.1016/j.ocemod.2004.08.002.

Shchepetkin, A. F., and McWilliams, J. C. 2009. Correction and Commentary for "Ocean Forecasting in Terrain-Following Coordinates: Formulation and Skill Assessment of the Regional Ocean Modeling System" by Haidvogel et al., J. Comp. Phys. 227, Pp. 3595-3624. Journal of Computational Physics 228(24): 8985–9000. http://dx.doi.org/10.1016/j.jcp.2009.09.002.

Swenson, E. M. 2003. Assessing the Potential Climate Change Impact on Salinity in the Northern Gulf of Mexico Estuaries: A Test Case in the Barataria Estuarine System. Integrated assessment of the climate change impacts on the Gulf Coast Region. GCRCC & LSU Graphic Series, Baton Rouge, LA: 131–50.

Twine, T.E., Kucharik, C.J., Foley, J.A. 2005. Effects of El Niño-Southern Oscillation on the climate, water balance, and streamflow of the Mississippi River basin. J. Clim. 18, 4840–4861.

Van Sickle, V. R., Barrett, B. B., Ford, T. B. 1976. Barataria Basin: Salinity changes and oyster distribution. Louisiana State University Center for Wetland Resource. Sea Grant Publication, Baton Rouge, LA, USA. https://repository.library.noaa.gov/view/noaa/8371.

Warner, J. C., Defne, Z., Haas, K., Arango, H. G. 2013. A wetting and drying scheme for ROMS. Computers and Geosciences, 58: 54–61. https://doi.org/10.1016/j.cageo.2013.05.004

Warner, J. C., Geyer, W. R., Lerczak, J. A. 2005. Numerical Modeling of an Estuary: A Comprehensive Skill Assessment. Journal of Geophysical Research: Oceans 110(5): 1–13. https://doi.org/10.1029/2004JC002691.

White, Eric D., Messina, F., Moss, L., Meselhe, E. 2018. Salinity and Marine Mammal Dynamics in Barataria Basin: Historic Patterns and Modeled Diversion Scenarios. Water 10(8).

Wiseman, W. J. Jr., Swenson, E. M. 1989. Modelling the effects of produced water discharges on

estuarine salinity. In: Donald F. Boesch and N. N. Rabalais (Eds), Environmental impact of produced water discharges in coastal Louisiana, 287 pp. https://deq.louisiana.gov/assets/docs/Water/EnvironmentalImpactProducedWaterDischarges inCoastalLouisiana.pdf.

Wiseman, W. J., Swenson, E. M., Power, J. 1990. Salinity Trends in Louisiana Estuaries."Estuaries 13(3): 265–71. https://doi.org/10.2307/1351917.

Zang, Z., Xue, Z. G., Xu, K., Bentley, S. J., Chen, Q., D'Sa, E. J., Ge, Q. 2019. A Two Decadal (1993–2012) Numerical Assessment of Sediment Dynamics in the Northern Gulf of Mexico. Water 11(5): 938. https://doi.org/10.3390/w11050938.

Table 1. Corresponding sites presented in this paper and USGS NWIS.

Sites in this paper	USGS NWIS
USGS 1	2951190901217
USGS 2	07380330
USGS 3	07380335
USGS 4	292800090060000
USGS 5	073802512
USGS 6	07380251
USGS 7	291929089562600
USGS 8	073802516
USGS 9	073802514
USGS 10	07380249
USGS 11	07380260

Fig. 1. Bathymetry (color) of (a) the Barataria Estuary; (b) the northern Gulf of Mexico (nGoM) domain, (c) Gulf of Mexico (GoM), and (d) computational meshes of the Barataria domain. The relative locations of the GoM, nGoM and Barataria Estuary are depicted in Fig. 1b and Fig. 1c by two solid black squares. The red dots in Fig. 1a represent the grids of point sources of the Davis Pond freshwater diversion (in the north) and the Mid-Barataria sediment diversion (MBSD, in the south). Locations of 11 USGS sites and one ADCP measurement site for model validation are denoted by black cross marks in Fig. 1a. The solid red lines in Fig. 1b and Fig. 1c indicate the mainstream of the Mississippi River. Note that the nGoM model provides the open boundary conditions to the Barataria Estuary model.
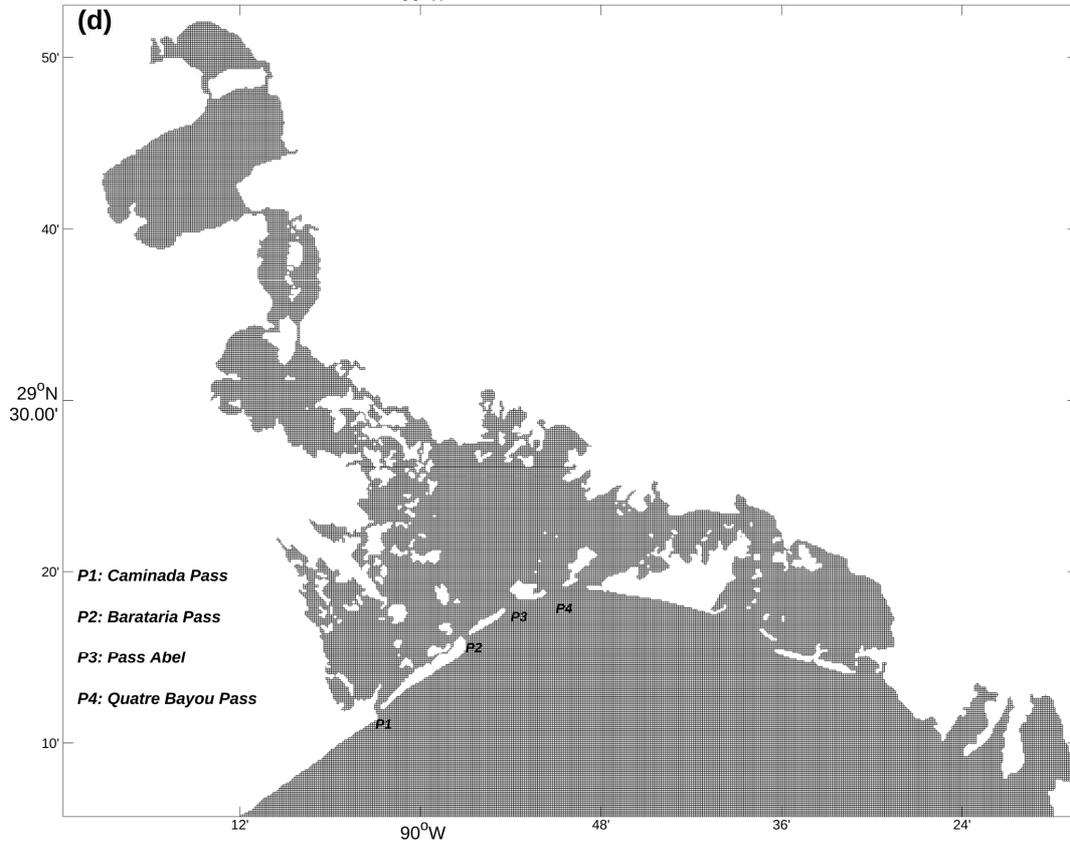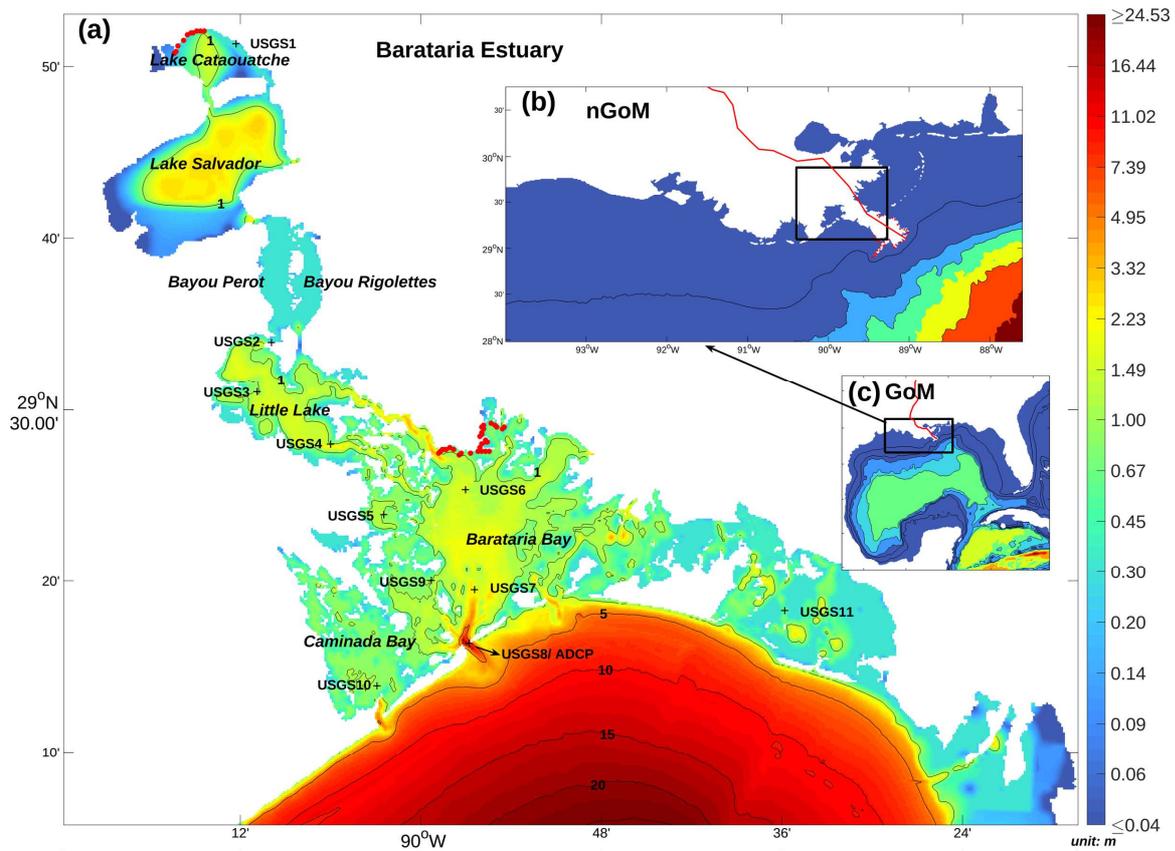
(a) Barataria Estuary

Lake Cataouatche
USGS1
Lake Salvador
Bayou Perot Bayou Rigolettes
USGS2
Little Lake
USGS3
USGS4
USGS6
USGS5
Barataria Bay
USGS9 USGS7
USGS11
Caminada Bay
USGS8/ ADCP
USGS10

unit: m

(b) nGoM

(c) GoM

(d)

P1: Caminada Pass

P2: Barataria Pass

P3: Pass Abel

P4: Quatre Bayou Pass

P3 P4
P2
P1

Fig. 2. (a) Distribution of density differences (in kg/m³) between the near-bottom and near-surface layers, (b) multi-year mean of depth-averaged salinity and current velocity over the period of interest (January 1, 2014~January 1, 2018), and multi-yearly (c) spring, (d) summer, (e) fall, and (f) winter mean of depth-averaged salinity and current velocity. The solid red lines indicate the isohaline of 8. Note that the current velocity in Fig. 2b-2f share the same vector scale as Fig. 2b.
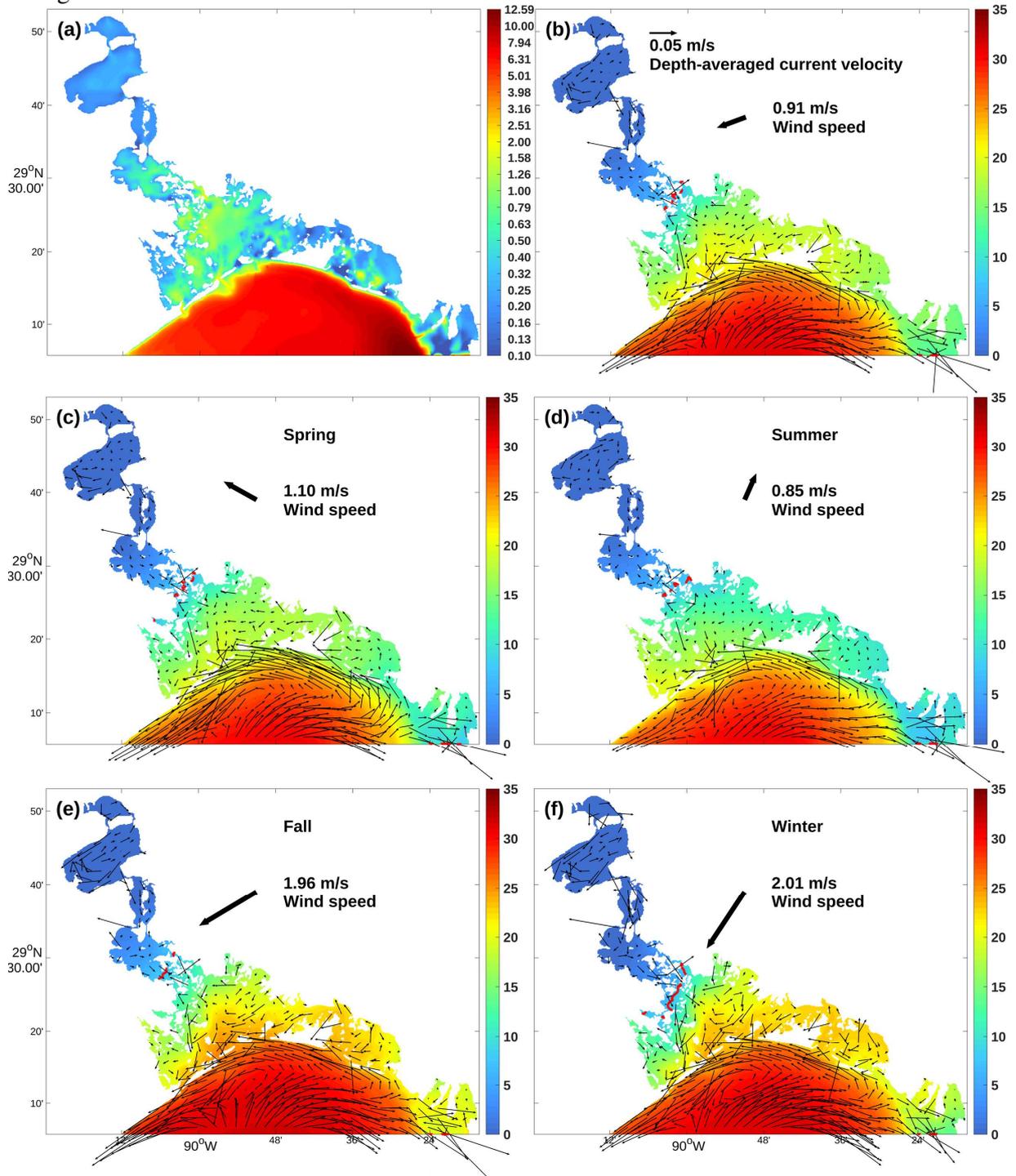
Fig. 3. (a) Daily time series of Davis Pond diversion discharges, upper-estuarine mean of depth-averaged salinity, (b) Mississippi River discharges, lower-estuarine mean of depth-averaged salinity, and entire-estuarine mean of depth-averaged salinity.
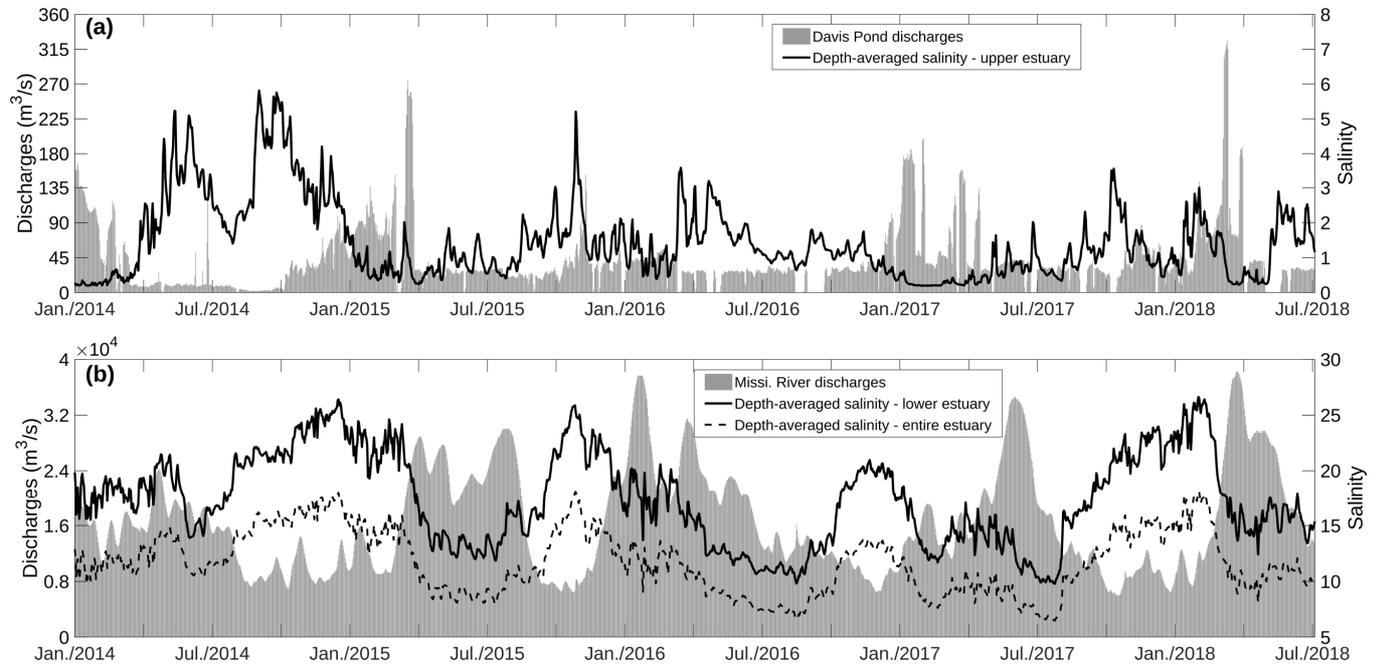
Fig. 4. Lead/lag correlation coefficients (CCs) of (a) Davis Pond diversion discharges and upper-estuarine salinity, and (c) of Mississippi River discharges and lower-estuarine salinity. CC figures of depth-averaged salinity and (b) Davis Pond diversion discharges with the discharges leading by 35 days, and (d) Mississippi River discharges with the discharges leading by 28 days. The solid black lines in (b) and (d) indicate CC isolines with an interval of 0.1. Note that only CCs over the 99% confidence level and CCs lower than -0.15 are shown in (b) and (d).
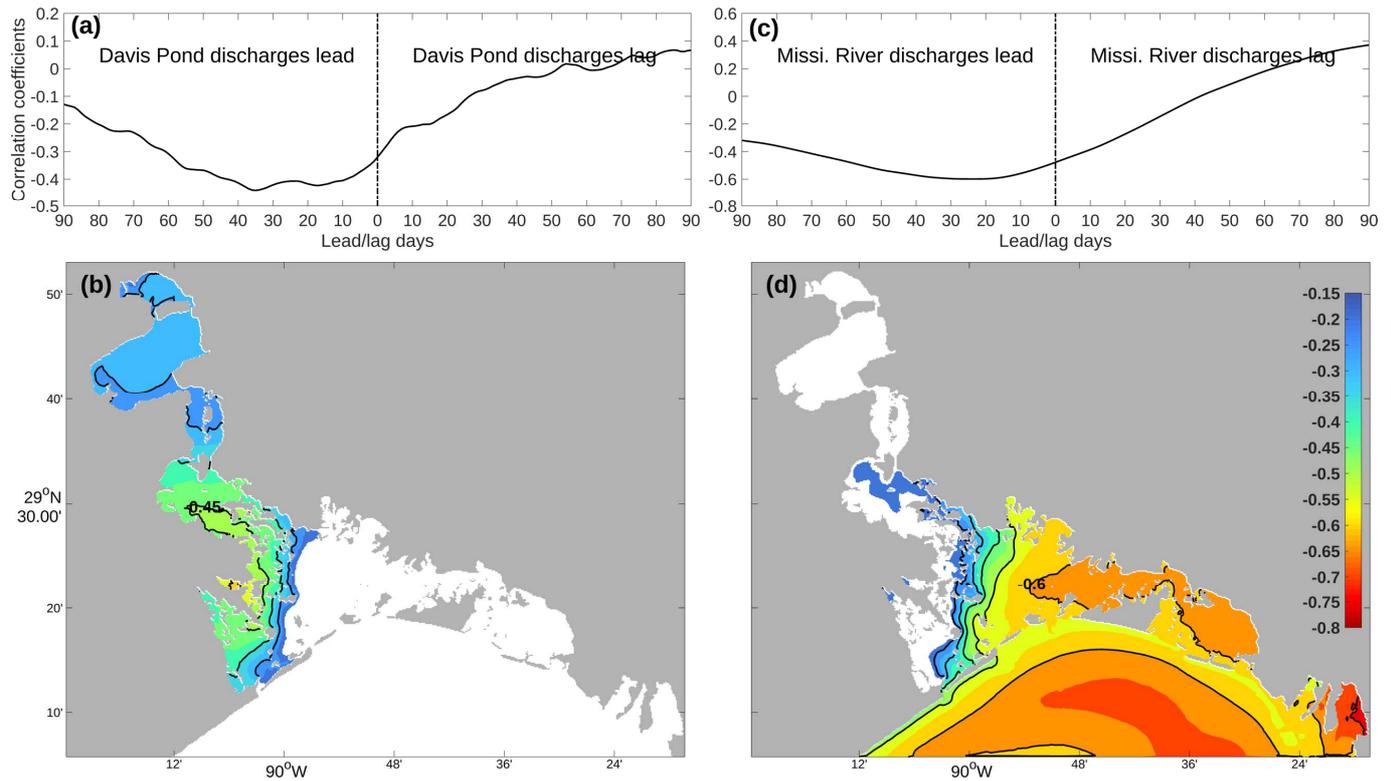
Fig. 5. Multi-yearly seasonal mean of depth-averaged salinity differences between half Mississippi River scenario and standard scenario (a, b, c, and d), double Mississippi River scenario and the standard scenario(e, f, g, and h), and MBSD scenario and the standard scenario (i, j, k, and l). The solid black lines indicate the isohalines of 0.
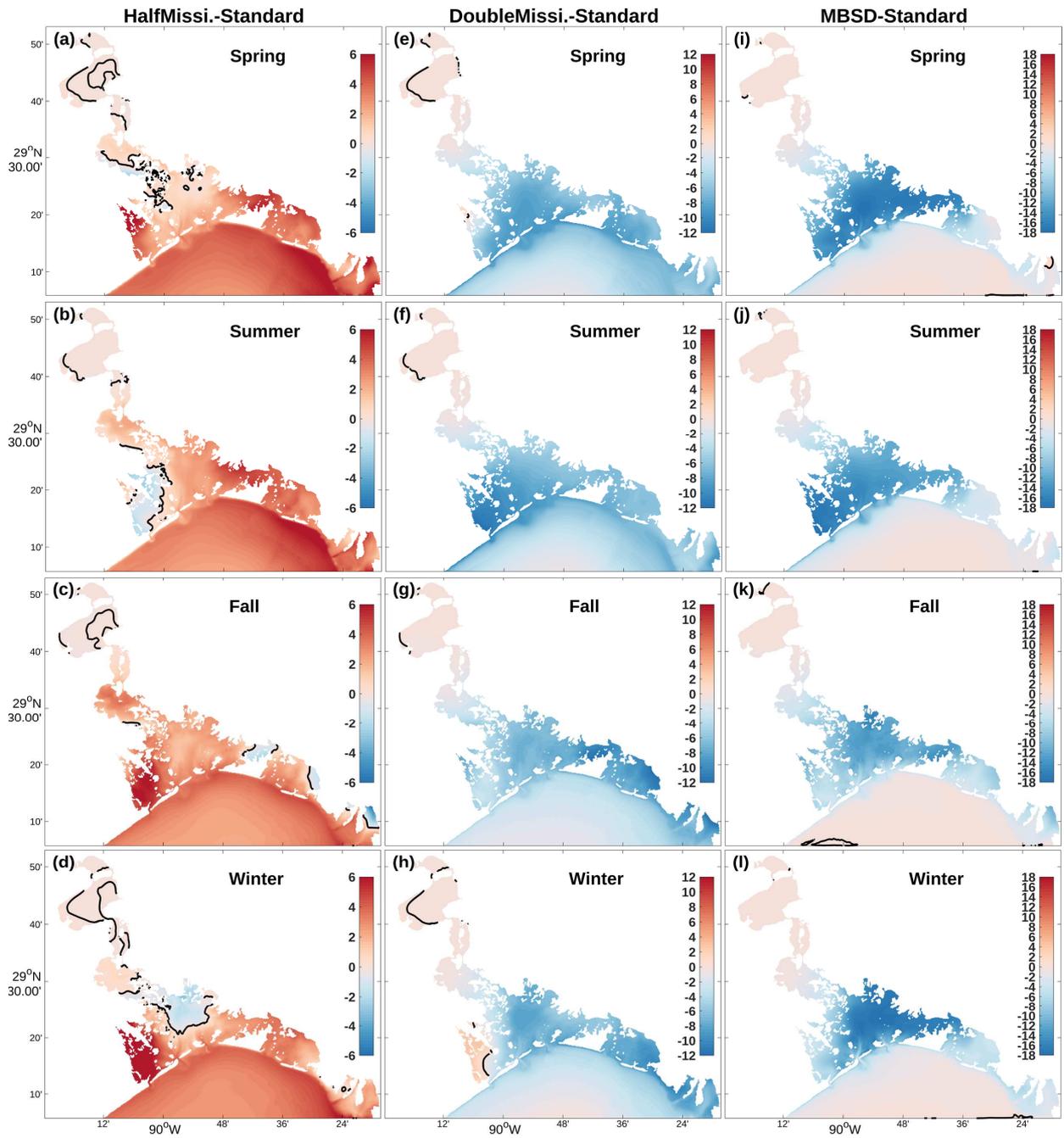
Fig. 6. Correlation coefficients of depth-averaged salinity and the Mississippi River discharges with the discharges leading by 28 days. The solid black lines indicate CC isolines with an interval of 0.1. Note that only CCs over the 99% confidence level and CCs lower than -0.15 are shown.
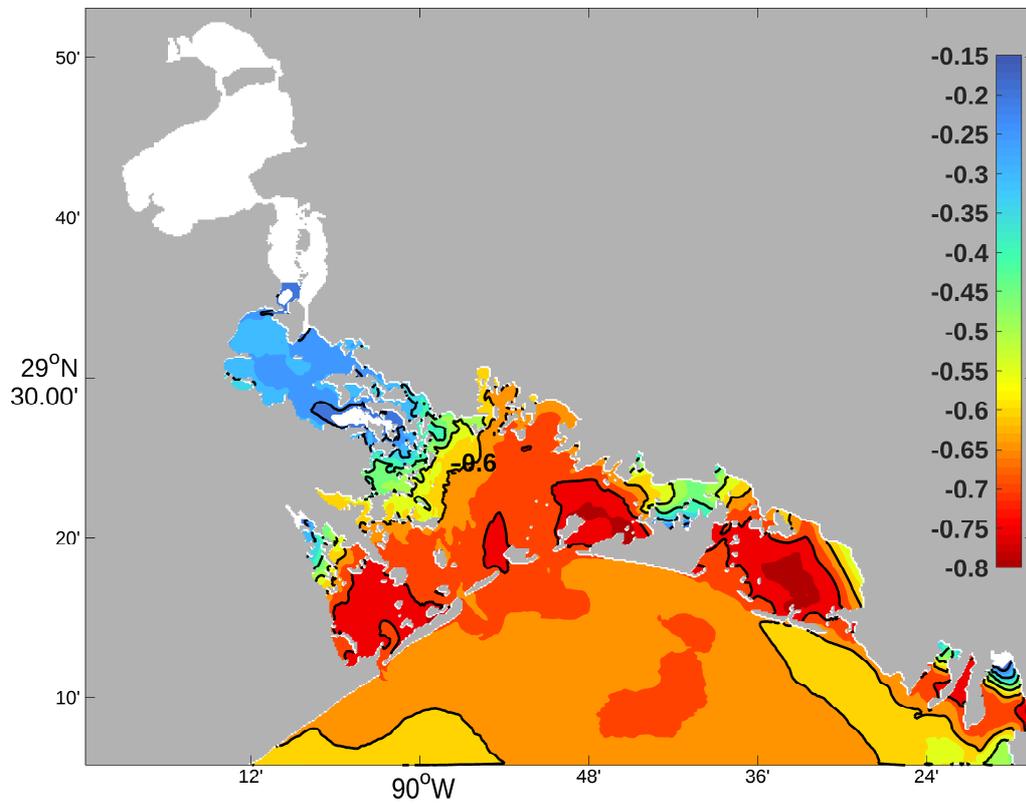
Fig. 7. (a) Daily time series of spatially averaged salinity over the entire estuary for standard scenario, two Mississippi River discharge scenarios, and MBSD scenario, and (b) daily time series of salinity percentage changes for different Mississippi River discharge scenarios and MBSD scenario relative to the standard scenario.